SECONDARY BASICS

TESLA SECONDARY SIMULATION PROJECT

Document pn2511, version 1.0e. See [1] for the latest revision of this document.

Warning This document has not been independently checked or peer reviewed by any authoritative body, so please exercise a due level of skepticism. The author welcomes criticism.

1. Introduction

The Tesla secondary supports a pattern of electrical resonances in which energy is exchanged cyclically between the magnetic field and the electric field of the coil. In general the behaviour of solenoids at very high frequency is complicated to analyse, requiring some sophisticated mathematics to apply Maxwell's equations in the presence of a helical conductor. Fortunately we do not need to tackle this in order to gain considerable insight into the operation of a solenoid as a Tesla secondary, which exploits only the lowest frequency modes in which the electric field lies along the axis of the coil. The free space wavelengths of these axial resonances are very large compared to the physical dimensions of a typical secondary coil, and this enables some valuable approximations to be applied. We can ignore direct coupling between the two fields and instead consider them to be coupled only through the induced movement of charges along the winding. Also we do not need to consider retarded potentials and thus we are able to describe the behaviour of the secondary in terms of inductances and capacitances coupling currents and voltages along the coil. This very much simplifies the analysis since we can reduce the coil description to a network of infinitesimal mutual reactances and proceed to form equations describing the coil by applying Kirchhoff's laws in a straightforward way. This approach was first set out in 1921 by Breit [2] and we follow very much the same lines. To begin our analysis we must first define the physical capacitances and inductances involved, which is the subject of the next two sections.

2. Physical Capacitance

Figure 2.1 shows a sample of electric flux paths emanating from an arbitrary point on the surface of a coil situated above a finite ground plane. Each of these flux paths represents a component of the field which we can replace with an equivalent capacitance, the size of which represents the ratio between the potential difference across the two ends of the flux path and the flux connecting the two points. To do this we must regard each point on the coil as an arbitrarily small area, so that the sample capacitances shown in the figure are infinitesimal.

Date: 25th November 2000.

Produced by Paul Nicholson as part of the Tesla Secondary Simulation Project, http://www.abelian.demon.co.uk/tssp/.

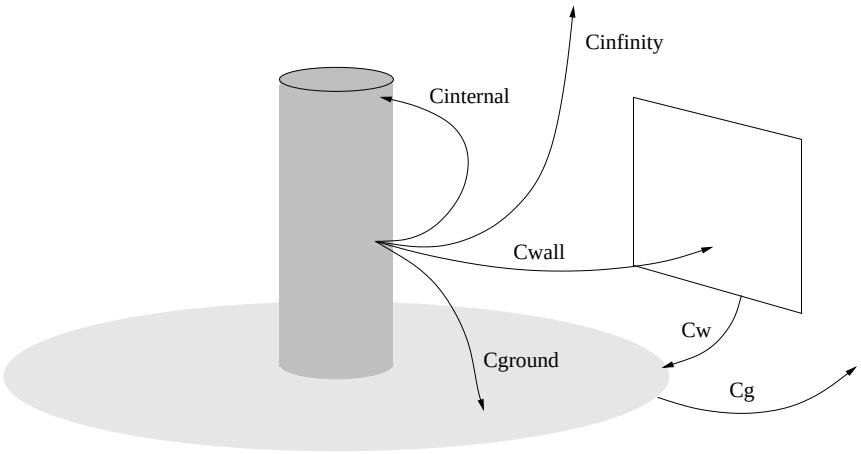

FIGURE 2.1. Types of capacitance around the coil

The capacitance C_{ground} represents flux passing between the point on the coil and the ground plane. If we declare the ground plane to be perfectly conducting, and if we ignore its self inductance, then the ground plane is at a uniform potential and C_{ground} can be considered the total capacitance from the sample point to the entire ground plane.

Different parts of the coil are at different potentials since they are connected by a conductor situated in a varying magnetic field. We must therefore introduce a capacitance $C_{internal}$ to represent flux passing between points on the coil. For each sample point such as the one shown, there is an infinite set of values for $C_{internal}$ corresponding to the capacitance between the sample point as source and each of the infinite number of destination points on the coil. Since there are also an infinity of sample points we can see that $C_{internal}$ takes the form of a scalar function of two position variables.

A capacitance such as C_{wall} exists between the sample point on the coil and objects in the vicinity. In general, such objects are at potentials determined by the ratio of C_{wall} to the capacitance C_w of the object to the ground plane. Since these objects are similarly coupled to all other points on the coil, they can place a parasitic contribution in parallel with $C_{internal}$. However, for simplicity, we'll assume that either C_w is much larger than C_{wall} or that all such objects are conductively grounded. Either way, this allows capacitances such as C_{wall} to be regarded as being in parallel with C_{ground}, and any parasitic contributions to $C_{internal}$ via C_{wall} will be shunted away.

Each sample point on the coil has a capacitance to infinity, represented by $C_{infinity}$. The displacement current return path for this capacitance is via the self capacitance to infinity of the ground plane itself, C_g. This latter is usually very much larger (in the case of the earth, several hundred μF) than $C_{infinity}$, so that, just as with C_{wall} we can also consider $C_{infinity}$ to be in parallel with C_{ground}. Note that we do not expect the field represented by $C_{infinity}$ to ever reach infinity. It is defined by considering the work done in bringing to the point a test charge from a reference potential of zero at infinity. It represents the charge supporting the far field of the coil and must be budgeted for in any resonator which is not

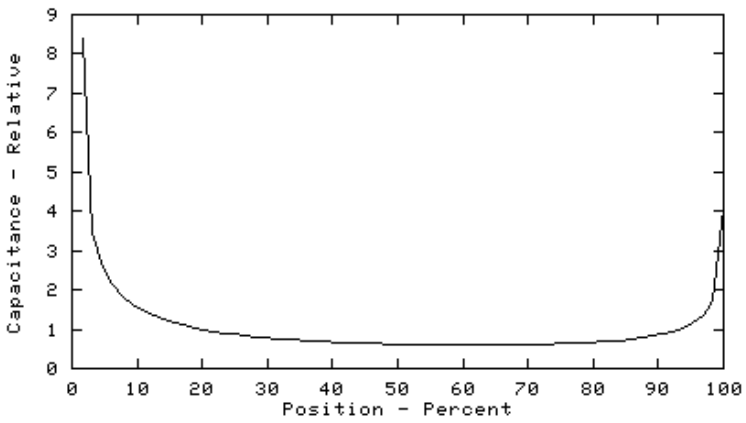

FIGURE 2.2. Typical external capacitance distribution of a Tesla secondary above a ground plane

completely contained. We are only entitled to describe it by a capacitance because of the long wavelength approximation accepted in the introduction [4].

We can summarise the physical capacitances of the resonator as just described, in terms of two scalar functions. For each infinitesimal section of the coil, with position x and length dx, the *external* capacitance is a scalar function of x and is defined as the parallel combination of C_{ground}, C_{wall}, and $C_{infinity}$, such that the total capacitance between the sample section and the ground plane is

$$C_{ext}(x)\,dx \tag{2.1}$$

By this definition $C_{ext}(x)$ is the external capacitance per unit length at the point x. Figure 2.2 shows the typical bathtub shape of $C_{ext}(x)$ for a coil without a top-load. The external capacitance rises steeply at the base of the coil, due to the close proximity of the end of the coil to the ground plane. A smaller rise occurs at the top due to the open end of the coil. When a top-load is fitted, this top-end rise in C_{ext} disappears due to the shielding effect of the top-load.

The *internal* capacitance can be described by a scalar function C_{int}, this time taking two position variables, defined so that the capacitance between an infinitesimal coil segment of length dx at position x and another section of length dy at position y is

$$C_{int}(x,y)\,dx\,dy \tag{2.2}$$

In accordance with the definition of capacitance, the function C_{int} is symmetric, ie $C_{int}(x,y) = C_{int}(y,x)$ and the diagonal values $C_{int}(x,x)$, which are undefined, are not used. Some sample slices through the internal capacitance function are shown in figure 2.3 Notice how the internal capacitance has a higher overall value when the end-most regions of the coil are involved. We'll see later that C_{int}, by coupling together remote regions of the coil has some interesting and significant effects on the operation of the secondary.

If a top-load is present, an additional scalar function is required in order to describe the capacitance between each sample point on the coil and the top-load. This is defined in a similar way to the others, so that the capacitance between the

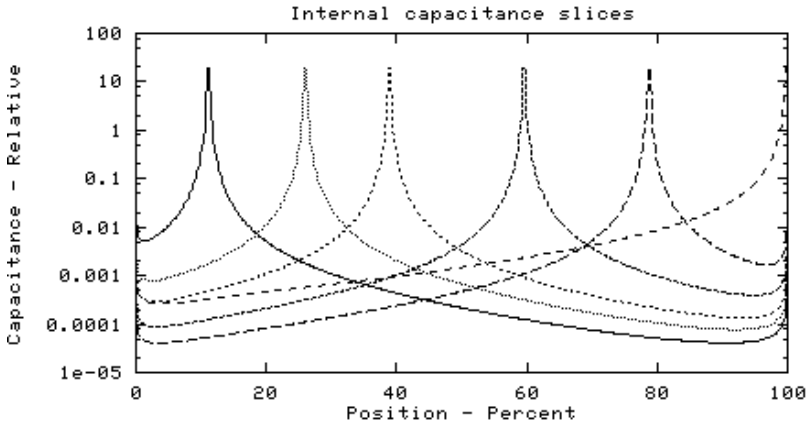

FIGURE 2.3. Typical internal capacitance distribution

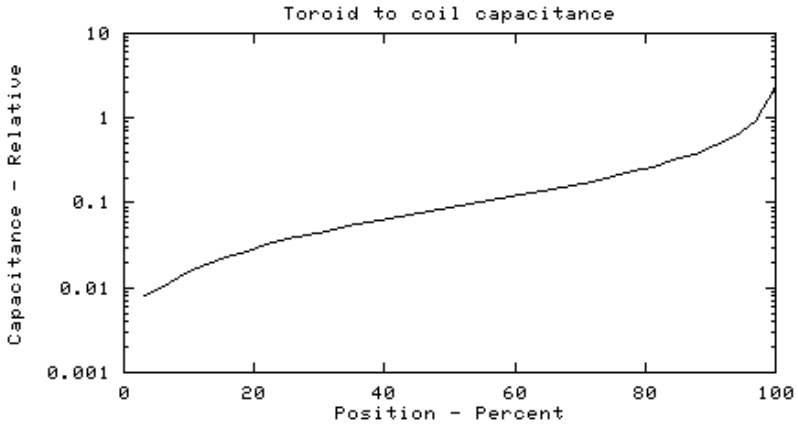

FIGURE 2.4. Typical toroid capacitance distribution

toroid and an infinitesimal coil section at position x of length dx is

$$C_{tor}(x)\,dx \tag{2.3}$$

Figure 2.4 shows the typical distribution of $C_{tor}(x)$. In addition to this distributed capacitance to the coil, the toroid will also have its own capacitance direct to the ground plane, which we'll represent by a single lumped capacitance C_{top}.

The functions which we have now introduced - C_{ext}, C_{int}, C_{tor}, and the top-load capacitance C_{top}, together provide a complete description of the electric field coupling of the coil. The picture of the resonator capacitance in terms of these functions is shown in figure 2.5. A sample point at position x is illustrated. Note that x can be taken to be either a distance along the coil, or a count of turns, or perhaps some other convenient measure. Another point y is shown in order to illustrate a specimen of $C_{int}(x, y)$ and both these points should be thought of as having an infinitesimal size dx and dy respectively. It may from time to time be

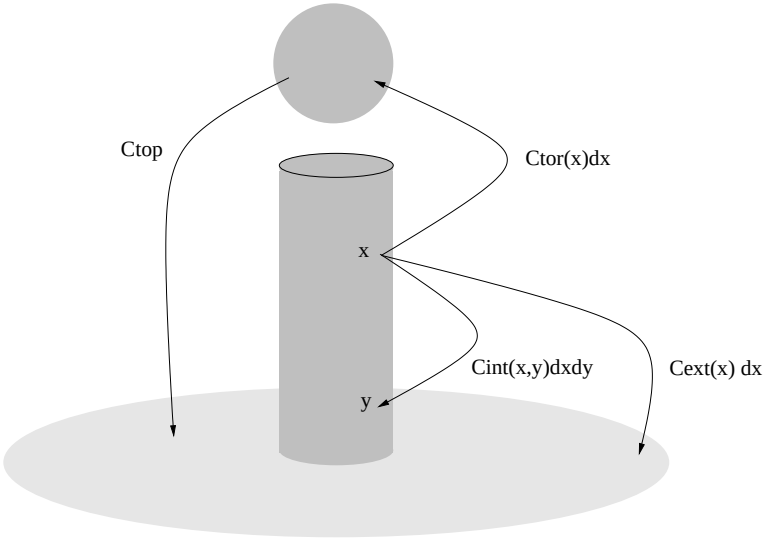

FIGURE 2.5. The physical capacitance functions

desirable to represent other electrodes in the resonator, for example strike rings and primary coupling coils. If the additional electrodes are conductively grounded, or can be considered so by virtue of having a large capacitance to ground, then their effect can be included in the C_{ext} function. If the electrodes are floating, then they will make a parasitic contribution to both internal and external capacitance, and again their effect can be included in C_{ext} and C_{int}. If the electrode is at an RF potential with respect to the resonator, then it may be necessary to an introduce an additional physical capacitance to describe its effect, either as a distributed function or a lumped total capacitance, much as we did for the top-load capacitance. This would be the case for example with a primary winding.

The physical capacitance functions can be determined numerically to arbitrary precision from the geometry of the coil and its surroundings by the solution of the Laplace equation or by a boundary element method [5]. In each case the physical capacitance distribution functions are obtained as matrices rather than continuous functions and the variable x is then a discrete position index and the infinitesimal length dx becomes a small but finite element size.

3. Physical Inductance

An infinitesimal portion of the coil at position x experiences an induced EMF proportional to its length dx. The magnitude of this EMF can be described in terms of the sum of an infinity of contributions from all the others points on the coil, each acting as a source current. The magnitude of each contribution is described by a mutual induction coefficient which we introduce as a scalar function of two position variables. The EMF induced across a section of length dx at position x due to a current $I(y)$ in a length of coil dy at position y is, [3]

$$M(x,y)\,dx\,dy\,\frac{dI(y,t)}{dt} \tag{3.1}$$

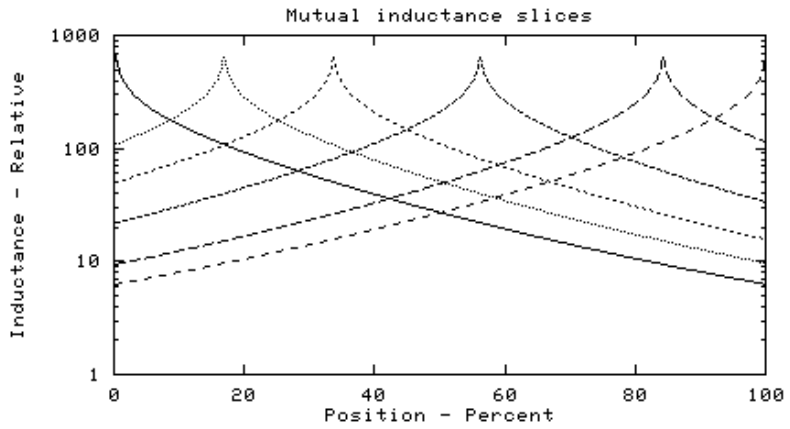

FIGURE 3.1. Typical mutual inductance distribution

Following from the definition of mutual inductance, the function $M(x, y)$ is symmetric, ie

$$M(x, y) = M(y, x) \tag{3.2}$$

and the self inductance of the infinitesimal elements are described by the diagonal terms $M(x, x)$. Figure 3.1 shows the relative mutual inductance along several slices through a typical mutual inductance profile function. The mutual inductance between turns separated by most of the length of the coil is about 1% of that which exists between neighbouring turns. It can be seen from this graph that the mutual inductance profile for any given turn is much the same as any other, and in fact for coils of uniform radius the function $M(x, y)$ can be replaced by one which takes a single argument,

$$M(x, y) \to M'(|x - y|) \tag{3.3}$$

but we will continue to use the more general $M(x, y)$. A similar mutual inductance function can be employed to describe the distributed coupling of a primary winding. In this case the primary is usually operated well below its lowest self-resonant frequency which allows us to treat its winding as a lumped inductor. We can for example define a function $M_p(x)$ such that

$$M_p(x)\, dx\, \frac{dI_p(t)}{dt} \tag{3.4}$$

is the EMF induced into the infinitesimal element of the secondary at x due to the primary current $I_p(t)$.

In practice, various sources of parasitic inductive coupling are potentially present, the two main ones being the formation of eddy current loops in the ground plane and in the top-load. The effect of these loops is to reduce the apparent self inductance of the solenoid and to reduce the Q factor. The magnitude of these effects is difficult to calculate and fortunately in most Tesla secondaries the modification of the self inductance due to coupling with eddy current loops is of order 1% or less and we can safely ignore it, which means that the functions $M(x, y)$ and $M_p(x)$ are sufficient to describe the magnetic behaviour of the coil.

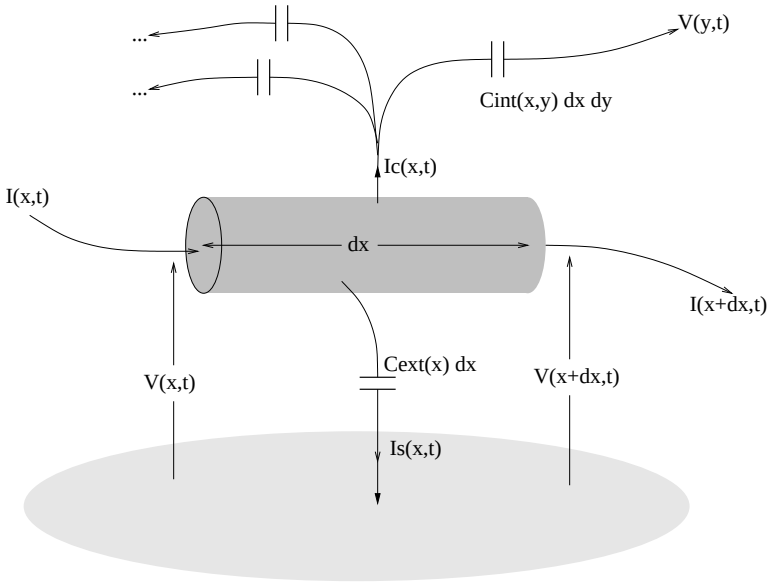

FIGURE 4.1. An infinitesimal coil section

When dealing with Tesla secondaries, the conductor size is small compared with the overall dimensions, which means that for computational purposes, $M(x, y)$ can be obtained with good accuracy from the coil geometry by calculating the mutual inductance between pairs of circular current filaments. It is also found that treating the primary conductor in terms of current filaments achieves reasonable accuracy despite the relatively larger conductor normally used [7].

4. The coupling equations

The previous two sections have defined the physical reactances of the resonator in terms of a number of scalar functions of position which, when taken together, completely describe the fields and their coupling in terms of the relationship between voltages and currents in infinitesimal regions of the coil. We'll now look in some detail at how the coupling takes place by examining the currents and voltages acting on a representative sample element of the coil. In order to concentrate on the reactances and coupling, we will not consider the mechanisms by which energy is dissipated in the resonator - the low loss typical of Tesla secondaries does not qualitatively affect any of the following loss-free analysis.

Figure 4.1 shows a sample element of the conductor at an arbitrary position x along the coil, and having an infinitesimal length dx. The current entering from the base of the coil is $I(x, t)$ and the current leaving towards the top of the coil is $I(x + dx, t)$. Similarly for the potentials, which change by an amount $dV(x, t)$ due to the induced EMF along the element. The first thing we'll do is consider the total charge Q stored on the surface of this element. Conservation of charge requires that the net conduction current entering this element matches the rate of increase of Q, ie [3]

$$\frac{dQ}{dt} = I(x, t) - I(x + dx, t) \tag{4.1}$$

The charge Q is responsible for maintaining the element at its potential $V(x,t)$ and Q is the sum of the charges associated with each of the infinitesimal capacitances shown in the figure. The charge necessary to set the potential $V(x,t)$ across the external capacitance $C_{ext}(x)\,dx$ is

$$Q_{ext} = C_{ext}\,dx\,V(x,t) \tag{4.2}$$

The internal capacitance, which is represented in figure 4.1 by a specimen contribution from another element of length dy at position y requires a charge

$$C_{int}(x,y)\,dx\,dy\,(V(x,t) - V(y,t)) \tag{4.3}$$

to maintain the potential across the specimen shown, and the total charge required at x to maintain the potential distribution across the entire internal capacitance is then the integral of this expression over all possible positions y along the length of the coil, ie

$$Q_{int} = dx \int_0^h C_{int}(x,y)(V(x,t) - V(y,t))\,dy \tag{4.4}$$

The two charges together account for the total charge on our element, ie

$$Q = Q_{ext} + Q_{int} \tag{4.5}$$

It's convenient to treat the rate of change of charge dQ/dt as a displacement current into the capacitance, since this allows Kirchhoff's laws to be applied. The external capacitance shunts a displacement current $I_s(x,t)$ to ground, given by

$$I_s(x,t) = \frac{dQ_{ext}}{dt} = C_{ext}(x)\frac{d}{dt}V(x,t)\,dx \tag{4.6}$$

and the corresponding definition for the total displacement current $I_c(x,t)$ into the internal capacitance is

$$I_c(x,t) = \frac{dQ_{int}}{dt} = \frac{d}{dt}\,dx \int_0^h C_{int}(x,y)(V(x,t) - V(y,t))\,dy \tag{4.7}$$

In terms of these two displacement currents, the rate of change of charge is

$$\frac{dQ}{dt} = I_s(x,t) + I_c(x,t) \tag{4.8}$$

and the charge conservation equation 4.1 then becomes

$$I_s(x,t) + I_c(x,t) + I(x+dx,t) - I(x,t) = 0 \tag{4.9}$$

which is just a statement of Kirchhoff's current law for the element.

Meanwhile, the EMF induced across this element due to current flow $I(y,t)$ in another element at position y is given by equation 3.1 and the total EMF induced in our sample element is the integral of this expression over all source current positions y along the coil. Given the direction established in the figure 4.1 for current flow through the element, the induced EMF will point in the opposite direction to the current flow, and so the differential increase in voltage on going from x to $x+dx$ will be

$$dV(x,t) = -\frac{d}{dt}\,dx \int_0^h M(x,y)I(y,t)\,dy \tag{4.10}$$

The two equations 4.9 and 4.10 are quite general and are the fundamental differential equations which must be satisfied by the currents and voltages at every point

on the coil at frequencies low enough for the long wavelength approximations to apply.

So far the time dependency has been shown explicitly but we will now simplify things by noting that since the equations are linear we can continue the analysis by looking only at solutions that have a sinusoidal variation with time, on the understanding that any arbitrary solution can be formed from the superposition of sinusoidal solutions of appropriate frequencies and phases. To do this we can replace the voltage $V(x,t)$ by a representative sinusoid $\sqrt{2}\bar{V}_\omega(x)\,e^{jwt}$ in which $\bar{V}_\omega$ is the phasor magnitude of the ω component, and is barred as a reminder that it is a complex phasor quantity. We will continue with this convention so that there is no confusion when we use the unbarred symbols later for peak amplitudes. The factor of $\sqrt{2}$ appears because the phasors $\bar{V}_\omega(x)$ are defined such that their magnitude is the effective or RMS value of the voltage. By switching to phasor quantities we can eliminate by cancellation the time dependency terms $\exp(j\omega t)$ altogether from equations 4.9 and 4.10 and introduce replacements parameterised by the angular frequency ω, as follows,

$$\bar{I}_s(x) = j\omega C_{ext}(x)\bar{V}(x)\,dx \tag{4.11}$$

$$\bar{I}_c(x) = j\omega\,dx \int_0^h C_{int}(x,y)(\bar{V}(x) - \bar{V}(y))\,dy \tag{4.12}$$

$$d\bar{V}(x) = -j\omega\,dx \int_0^h M(x,y)\bar{I}(y)\,dy \tag{4.13}$$

in which we have quietly dropped the ω subscript from the phasor magnitudes $\bar{V}(x)$ and $\bar{I}(x)$ and we must remember that these quantities refer to a single frequency component. Equation 4.13, together with the charge conservation equation, which is now

$$\bar{I}_s(x) + \bar{I}_c(x) + d\bar{I}(x) = 0 \tag{4.14}$$

constitute a complete set of differential equations, the solution of which for a given ω gives the current and voltage phasors $\bar{V}(x)$ and $\bar{I}(x)$ for that component for the entire coil, and these equations are satisfied independently for each frequency component.

If a top-load is present, an additional displacement current $\bar{I}_t$ - not shown on the diagram - leaves the element for the toroid, and we have

$$\bar{I}_t(x) = j\omega C_{tor}(x)(\bar{V}(x) - \bar{V}(h))\,dx \tag{4.15}$$

in which we assume that the toroid is connected to the top of the coil and thus has potential $\bar{V}(h)$. This simply adds another term into 4.14 and other electrodes at RF potentials can be treated similarly.

We'll now substitute 4.11 and 4.12 into the charge conservation equation 4.14 and rearrange a bit to get the equations in a slightly more compact form,

$$\frac{d\bar{I}(x)}{dx} = -j\omega C_{ext}(x)\bar{V}(x) - j\omega \int_0^h C_{int}(x,y)(\bar{V}(x) - \bar{V}(y))\,dy \tag{4.16}$$

$$\frac{d\bar{V}(x)}{dx} = -j\omega \int_0^h M(x,y)\bar{I}(y)\,dy \tag{4.17}$$

The reader may recognise these as being similar to the differential equations which apply to a uniform transmission line, the significant difference being the presence of the integrals on each right hand side. These integrals describe a type of coupling which is negligible in, say, a coaxial cable. They represent longitudinal coupling occurring through the mutual inductance and internal capacitance. If the Tesla coil were continuously deformed - increased in length and reduced in radius - so that it gradually became a long thin straight wire, the C_{int} terms would gradually become small compared with C_{ext}, eventually rendering the longitudinal coupling through C_{int} negligible. At the same time the non-diagonal terms in $M(x,y)$, which are the ones responsible for the inductive longitudinal coupling, will also become negligible, leaving behind only the diagonal self inductance terms $M(x,x)$. The end result of this deformation is an open wire non-uniform line with the equations

$$\frac{d\bar{I}(x)}{dx} = -j\omega C_{ext}(x)\bar{V}(x) \tag{4.18}$$

$$\frac{d\bar{V}(x)}{dx} = -j\omega M(x,x)\bar{I}(x) \tag{4.19}$$

in which the diagonal terms $M(x,x)$ are seen to be to the self inductances per unit length. These are the standard equations of a transmission line valid in the absence of longitudinal coupling. A great many results follow from these due to the essential simplicity of the system, in which the current and voltage at a point on the coil are dependent only on the voltage and current respectively at the same point. However, once we introduce the non-local terms of the longitudinal coupling, it becomes hard, if not impossible, to solve the equations analytically, although some progress can be made for a coil of infinite length. The problem of solving 4.16 and 4.17 can however be tackled numerically without difficulty by replacing the integrals and differentials with finite sums and differences, and employing a discrete form of the physical reactance distributions to obtain the equations in matrix form, which are then solved by Gaussian elimination [6].

It should be noted that the coupling equations derived so far are valid for a solenoid in any configuration as we have not yet introduced any boundary conditions to restrict them specifically to Tesla coils. We can represent the normal Tesla secondary configuration which has the base of the coil connected to the ground plane by the constraint $\bar{V}(0) = 0$ and the open circuit top of the coil by $\bar{I}(h) = 0$. With these two extra equations, the solutions are constrained to only those possible on a grounded base Tesla coil with an open top. Alternatively the toroided top is represented by

$$\bar{I}(h) = j\omega C_{top}\bar{V}(h) + j\omega \int_0^h C_{tor}(\bar{V}(h) - \bar{V}(x))\,dx \tag{4.20}$$

where C_{top} is the capacitance of the top-load to the ground plane and the integral describes the total displacement current entering the toroid to coil distributed capacitance.

5. The resonances

We are particularly interested a certain class of solutions of 4.16 and 4.17 - those which correspond to the resonances. Suppose for a moment that a solution exists in which all the voltages $\bar{V}(x)$ are in phase with one another. Then since each term

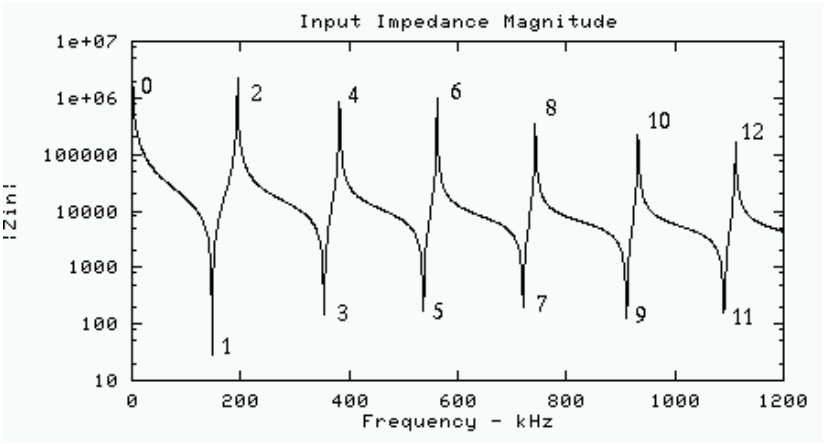

FIGURE 5.1. The input impedance spectrum

in the right hand side of 4.16 has a coefficient of j, all the current differentials, and therefore the all the currents $\bar{I}(x)$, are also in phase with one another and 90 degrees out of phase with the voltages. This uniform-phase current distribution, when inserted into the right hand side of 4.17 reproduces the original uniform phase proposed for the voltage distribution. The solutions of the equations which have this character are called resonances and the values of ω for which these occur are the resonant angular frequencies. The resulting uniform-phase voltage and current distributions are called standing waves. This phenomena is not peculiar to Tesla coils, but is a characteristic of any conductor which has distributed inductance and capacitance - in other words any conductor of finite size.

At the resonances, the voltage and current amplitudes take on a particularly simple form: At two points in each cycle the entire coil voltage is momentarily zero and simultaneously the current along the coil is at its maximum instantaneous value. At two other points, 90 degrees away in phase, the coil current is momentarily uniformly zero and the voltages reach their maximum instantaneous values all along the coil. Thus at resonance the stored energy is transferred completely from one field to another twice in each cycle. At frequencies in between the resonances, these descriptions don't apply, and there is never a point in the AC cycle at which the entire energy is stored in just one of the fields. Thus, only at the resonances is the maximum voltage achieved for a given stored energy.

We can explore the location of these resonances in the frequency domain by solving the equations 4.16 and 4.17 for a wide range of values of ω and plotting the results on a graph. A convenient parameter to plot is the ratio $\bar{V}(0)/\bar{I}(0)$ which is the complex impedance seen between the base of the coil and the ground plane. The magnitude of this impedance is shown in figure 5.1 plotted against frequency $\omega/2\pi$ for a typical secondary coil. The resonances are revealed by the peaks and dips of the impedance response. These are numbered on the impedance graph and the reasoning behind the choice of numbers will be explained shortly. In fact the equations modeled to produce this graph are slightly extended from those given in 4.16 and 4.17 in order to include the effect of losses. If the loss-free equations were modeled, the dips would extend down to zero ohms, and the peaks would rise to

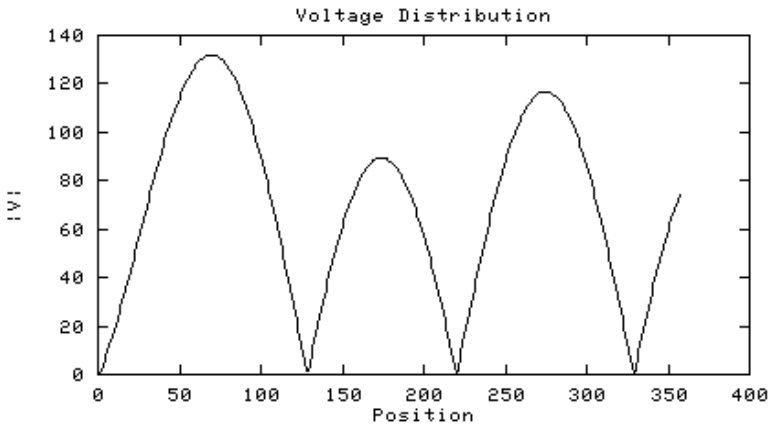

FIGURE 5.2. Voltage distribution of the 7th resonance

infinity. When the grounded-base boundary condition $\bar{V}(0) = 0$ corresponding to the normal Tesla secondary configuration is applied, the even numbered resonances are suppressed and only the odd numbered solutions are available. Conversely, if an open-circuit base condition $\bar{I}(0) = 0$ is applied, as in a bipolar coil, the odd numbered resonances are suppressed instead. Tesla coil operation normally exploits the shorted-base resonance numbered 1, or sometimes the open-circuit resonance 2.

To explain the numbering scheme, we'll take a look at the voltage profile $|\bar{V}(x)|$ corresponding to the resonance number 7. The standing wave profile consists of a number of peaks, and in terms of travelling waves reflecting from the ends and mutually interfering, the peaks each have a width of half a wavelength. Thus the example shown suggests the coil has an electrical length of 7 quarter wavelengths and with this in mind we have numbered the resonances according to how many quarter wavelengths are present. Note that when top-loading capacitance is present at the end of the coil, the final quarter-wave of the standing wave will appear to be truncated, the missing electrical length being provided by the top-load reactance itself.

It is clear from the input impedance graph that the resonant frequencies are not harmonically related. The even numbered resonances are only a little higher in frequency than the odd numbered resonance immediately beneath. From about the 4th resonance upwards they exhibit an approximately constant frequency step between consecutive even numbered resonances, and similarly between the odd numbered. The longitudinal coupling due to mutual inductance, and particularly the internal capacitance, in combination with the finite length of the coil, is responsible for the variation of velocity with frequency which lies behind these intervals.

6. AMPLITUDE PROFILES

In the previous section we have seen that at the resonances all the voltages $\bar{V}(x)$ share a common phase, and so do all the currents $\bar{I}(x)$, with the two phases separated by 90 degrees. With the current and voltage polarities chosen in figure 4.1, the current phase leads the voltage phase. We can exploit the uniform phase to

make another major simplification in which we replace the complex phasor amplitudes with scalar magnitudes. We'll start with the equation 4.17 for the differential voltage along the coil. This is an equality in complex quantities and therefore it must be satisfied separately by the real and imaginary components on each side. We can for example write

$$\frac{d\Re(\bar{V}(x))}{dx} = -\omega \int_0^h M(x,y)\Re(j\bar{I}(y))\,dy \tag{6.1}$$

Now the reference phase for the phasor quantities involved in a set of equations can be chosen arbitrarily. Let's say that for the particular resonance occurring at angular frequency ω the voltages are all entirely real, ie we are choosing a phase reference such that the relative phase of all the voltages is zero. We can see then from equation 6.1 that the currents are all entirely imaginary. With our choice of phase reference, we can write down the following two relationships between the complex phasor amplitudes and the peak magnitudes:

$$\begin{aligned} V(x) &= \sqrt{2}\Re(\bar{V}(x)) \\ I(x) &= \sqrt{2}\Im(\bar{I}(x)) \\ &= -\sqrt{2}\Re(j\bar{I}(x)) \end{aligned} \tag{6.2}$$

where we now begin to use the unbarred quantities specifically for the peak magnitudes. Using these equations to replace the phasors $\bar{V}(x)$ and $\bar{I}(x)$ in equation 6.1 gives

$$\frac{dV(x)}{dx} = \omega \int_0^h M(x,y)I(y)\,dy \tag{6.3}$$

and the same substitutions into the real part of equation 4.16 gives

$$\frac{dI(x)}{dx} = -\omega C_{ext}(x)V(x) - \omega \int_0^h C_{int}(x,y)(V(x) - V(y))\,dy \tag{6.4}$$

With these two equations we now have scalar relationships between the current and voltage peak amplitudes which are valid only at resonant angular frequencies ω since we have obtained them by making use of the phase relationships which exist between the phasor quantities only at resonance. Since 6.3 and 6.4 are linear we are free to take $V(x)$ and $I(x)$ as either peak or RMS values. Examination of these differential equations reveals a number of general characteristics of the amplitude profiles which we'll look at from the point of view of the single quarter-wave resonance. Figure 6.1 shows the relative current and voltage amplitudes for an example secondary. The amplitudes are normalised to a base current and top voltage of 100%. These profiles differ quite a bit from those found in a uniform transmission line with no longitudinal coupling. Significantly, the current maxima occurs some distance above the base of the coil - in this example 34%, but always below the midpoint, as we shall see later.

A number of features can be noted from this graph. Firstly, the current is always positive - there are no zero crossings by definition, since this is a single quarter-wave resonance. Therefore the right hand side of equation 6.3 is always positive and as a result, $V(x)$ is monotonically increasing throughout the length of the coil, which implies that the voltage maximum is always right at the top. Secondly, the current remains significant all the way along the coil - it falls below 40% of I_{base} only in the top 5% of the coil. Thirdly, there is a point on the coil - in this case at about

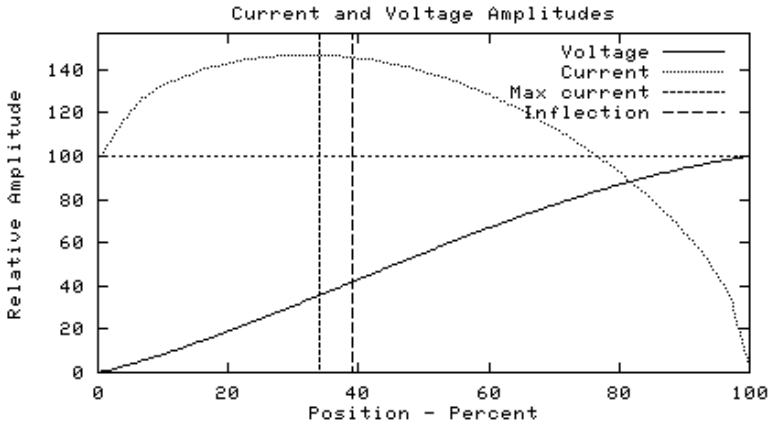

FIGURE 6.1. An example current and voltage profile

39% height, below which the voltage curve is concave and above which it is convex. This *point of inflection* in the voltage curve is invariably located a little higher up the coil than the current maximum, and at this point the voltage gradient is higher than anywhere else on the secondary. Fourthly, the current rises, in this case, to a maximum around 40% higher than I_{base}. The origin of this maximum can be seen from equation 6.4. The term $\omega C_{ext}(x)V(x)$ on the right is always positive, since as we've already noted, $V(x)$ is always positive. If this were the only term on the right, then $dI(x)/dx$ would be negative all along the coil, and the current would be monotonically decreasing from a maximum of I_{base} at the base. However the longitudinal term arising from C_{int} alters this picture. In the upper part of the coil the terms (V(x) - V(y)) are positive more often than negative, and in view of the symmetry and approximate uniformity of $C_{int}(x, y)$ this observation applies to the integral as a whole. Thus in the upper part of the coil, the second term is of the correct sign to assist the first term in enforcing a monotonically decreasing current. At some point lower down the coil however, the value of the integral changes sign and if the C_{int} is large enough we will see a positive $dI(x)/dx$ for part of the lower half of the coil, thus giving rise to a current maximum within the coil rather than at the base. The current maximum occurs at a position x_{imax} in which the two terms on the right of 6.4 cancel one another, ie when

$$C_{ext}(x_{imax})V(x_{imax}) = -\int_0^h C_{int}(x_{imax}, y)(V(x_{imax}) - V(y))\, dy \tag{6.5}$$

Below the current maximum there is more displacement current entering the coil via C_{int} from higher up, than there is current leaving the coil to ground via C_{ext}. In fact the particular coil to which figure 6.1 relates has a h/d ratio of unity and was placed high off the ground - a choice intended to maximise the effects of internal capacitance in order to clearly demonstrate the elevated current maximum. In a more typical, larger h/d configuration, with the coil base less than one coil-length above the ground plane, the increased external capacitance reduces the current maximum in both amplitude and elevation. Figure 6.2 shows an example of a coil with $h/d = 3$. Here we see the voltage inflection point occurs at 28% and the

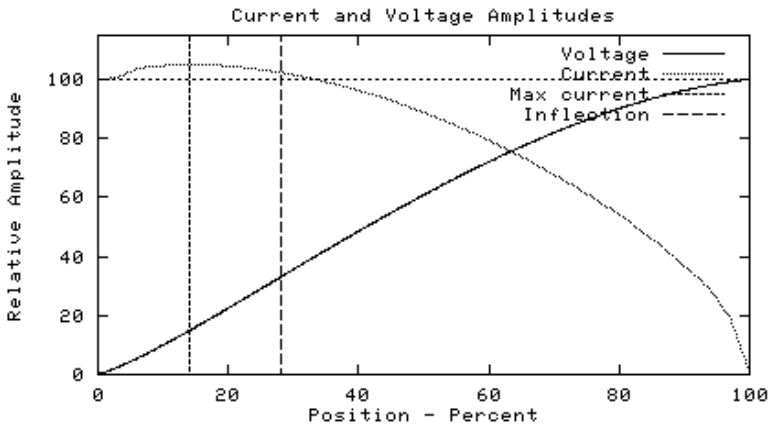

FIGURE 6.2. Profiles of a more typical secondary

current maximum at 14% height. In general, as the h/d ratio is reduced, or the coil is raised further above its ground plane, the location of the current maximum and the voltage inflection point move upwards towards the middle of the coil.

The inflection point is a significant position on the Tesla secondary since it identifies the location of highest voltage gradient. Its location some way above the current maximum can be understood by examining 6.3. If the magnitude of $M(x, y)$ was constant along the coil, right up to the ends, we can see that the maximum voltage gradient would coincide with the maximum position of $\bar{I}$. However the absence of turns continuing beneath the base of the coil reduces the average value of $M(x, y)$ as x approaches the base. This average increases to a peak exactly at the mid-point of the coil and the resulting slope in the average size of $M(x, y)$ has the effect of making the right hand side of 6.3 greatest somewhere above the maximum of $I(y)$, displacing the point of maximum voltage gradient a little above the point of maximum current, but not higher than the mid-point. For a coil operating in free space or at high elevation, the capacitance is dominated by C_{int} and both the inflection point and the current maximum converge towards the mid-point of the coil. As we've seen in these two examples, the location of the inflection point and the current maximum both fall as the h/d ratio is increased.

7. Equivalent Reactances

When considering the operation of the secondary in the context of the Tesla system as a whole, it is often convenient to represent the overall characteristics of the secondary in terms of quantities which can be incorporated into circuit theory calculations. For this reason we define a number of useful *equivalent reactances* and explain their use. These equivalents can only be defined for a single resonant frequency at a time, and unless otherwise stated this can be assumed to be that of the quarter-wave resonance. We will make frequent use of the coil base current and top voltage so we will introduce the abbreviations

$$\begin{aligned} \bar{I}_{base} &= \bar{I}(0) \\ \bar{V}_{top} &= \bar{V}(h) \end{aligned} \tag{7.1}$$

We will also use the corresponding unbarred quantities when considering just the scalar peak amplitudes, and on these occasions the equations will often be valid regardless of whether we take the amplitudes to be RMS or peak values, so long as we stay with a choice of one or the other. We will now define a number of equivalent reactances and then go on to show how these are related to each other and to ω, $\bar{V}_{top}$, and $\bar{I}_{base}$.

7.1. **DC capacitance.** If we apply a potential to the base at an arbitrarily low frequency then the voltage along the coil can be considered uniform. Under these conditions all the infinitesimal external capacitances $C_{ext}(x)dx$ can be regarded as acting in parallel and consequently the total capacitance seen between the base terminal and the ground plane at low frequency is given by the integral of all these along the coil,

$$C_{dc} = \int_0^h C_{ext}(x)\,dx \tag{7.2}$$

This quantity is fairly easy to measure and provides a useful cross-check on computed values of the external capacitance distribution.

7.2. **Equivalent shunt capacitance.** The total current reaching the ground plane from the coil is given by the integral of all the infinitesimal contributions $\bar{I}_s(x)$. By charge conservation, this total must equal the base current of the coil, therefore we have

$$\bar{I}_{base} = \int_0^h \bar{I}_s(x) = j\omega \int_0^h C_{ext}(x)\bar{V}(x)\,dx \tag{7.3}$$

We can choose to pretend that this entire current flow comes from a single lumped capacitor charged to $\bar{V}_{top}$, which we'll call the equivalent shunt capacitance C_{es}, with the understanding that the equivalent is obtained by referring all the shunt capacitance to the top of the coil. We could have chosen any other point, but the accessible $\bar{V}_{top}$ is the one we are most interested in. Thus we choose to define C_{es} by

$$\bar{I}_{base} = j\omega C_{es}\bar{V}_{top} \tag{7.4}$$

and eliminating $\bar{I}_{base}$ by substituting from 7.3 gives

$$C_{es} = \frac{1}{\bar{V}_{top}} \int_0^h C_{ext}(x)\bar{V}(x)\,dx \tag{7.5}$$

which describes a summing of the external capacitance distribution with each contribution weighted by the normalised voltage at that point. The equivalent shunt capacitance can be measured by taking simultaneous measurements of I_{base} and V_{top}, from which

$$C_{es} = \frac{1}{\omega}\frac{I_{base}}{V_{top}} \tag{7.6}$$

At the quarter-wave resonance, C_{es} is usually less than 70% of the value of the DC capacitance.

7.3. **Equivalent energy capacitance.** It is often useful to know how much energy needs to be stored in the resonator to obtain a given V_{top}. To this aim we consider the energy stored in the resonator at a point in the cycle where all the energy is stored in the capacitance. At this instant the energy stored in the each infinitesimal element of external capacitance $C_{ext}(x)\,dx$ is given in terms of the peak voltage across it, by

$$\frac{1}{2}C_{ext}(x)V(x)^2\,dx \tag{7.7}$$

and so the total energy stored in external capacitance is the integral of this over all possible positions x,

$$E_{ext} = \frac{1}{2}\int_0^h C_{ext}(x)V(x)^2\,dx \tag{7.8}$$

Similarly with the internal capacitance, the capacitance $C_{int}(x,y)\,dx\,dy$ between infinitesimal elements at x and y stores an energy

$$\frac{1}{2}C_{int}(x,y)(V(x)-V(y))^2\,dx\,dy \tag{7.9}$$

and integrating this over all possible combinations of x and y gives the total energy stored in the internal capacitance as,

$$E_{int} = \frac{1}{4}\int_0^h\int_0^h C_{int}(x,y)(V(x)-V(y))^2\,dx\,dy \tag{7.10}$$

where an extra factor of 2 appears in the denominator since the integral counts each contribution twice. The total stored energy is the sum of these two expressions and we can ask what single lumped capacitance would store this same energy if charged to V_{top}. The result is the equivalent energy capacitance C_{ee} defined by

$$\frac{1}{2}C_{ee}V_{top}^2 = E_{ext} + E_{int} \tag{7.11}$$

and thus C_{ee} is given by

$$\begin{aligned} C_{ee} =& \frac{1}{V_{top}^2}\int_0^h C_{ext}(x)V(x)^2\,dx \\ &+ \frac{1}{2V_{top}^2}\int_0^h\int_0^h C_{int}(x,y)(V(x)-V(y))^2\,dx\,dy \end{aligned} \tag{7.12}$$

which can be thought of as a weighting of the capacitance contributions by the normalised square of the voltage across them. This capacitance can be used to obtain the top voltage from the stored energy. For example, if an amount of energy $0.5C_{pri}V_{pri}^2$ is introduced from a coupled primary resonator, the peak voltage achieved at the top of the secondary can be seen to be

$$V_{top} = V_{pri}\sqrt{\frac{C_{pri}}{C_{ee}}} \tag{7.13}$$

which is a familiar formula to Tesla coil builders, although we can now be quite specific about which capacitance to use. C_{ee} also finds an important use in the description of the output impedance of the resonator. It is found that C_{ee} is slightly lower than C_{es} for coils with medium or larger h/d ratio. In coils with small h/d the energy storage due to internal capacitance can become very significant and C_{ee} will exceed C_{es}.

At higher resonances the energy storage due to C_{int} increases dramatically, effectively discouraging the use of these higher modes for Tesla coils. The internal capacitance, and therefore C_{ee}, can be reduced by splitting the secondary, as in a secondary-tertiary combination or a split bipolar secondary.

7.4. **DC inductance.** We see from equation 4.13 that the EMF induced across an element of length dx at position x is given by the integral of all the contributions due to an infinity of source currents in the rest of the coil, so that the differential voltage is

$$\frac{d\bar{V}(x)}{dx} = -j\omega \int_0^h M(x,y)\bar{I}(y)\,dy \tag{7.14}$$

The integral of this differential voltage over the length of the coil must equal the top voltage, ie

$$\bar{V}_{top} = \int_0^h \frac{d\bar{V}(x)}{dx}\,dx = -j\omega \int_0^h \int_0^h M(x,y)\bar{I}(y)\,dy\,dx \tag{7.15}$$

If a current is passed through the coil at a sufficiently low frequency, the currents all along the coil can be considered equal to $\bar{I}_{base}$. With this value providing all the current terms in 7.15, we have for the total voltage induced across the whole coil,

$$\bar{V}_{top} = -j\omega \int_0^h \int_0^h M(x,y)\bar{I}_{base}\,dx\,dy \tag{7.16}$$

From this we can see that the DC or low frequency inductance is given in terms of $M(x,y)$ by

$$L_{dc} = \int_0^h \int_0^h M(x,y)\,dx\,dy \tag{7.17}$$

which is the straight sum of all the components in $M(x,y)$. For the Tesla coil, the DC inductance is calculated quite accurately by Nagaoka's formula and the definition of L_{dc} enables a calculated mutual inductance profile to be checked against a straightforward measurement.

7.5. **Equivalent series inductance.** At higher frequencies the current can no longer be considered uniform along the coil and the top voltage is given in terms of the current by 7.15. We can define an equivalent lumped inductance which will induce this same total voltage when carrying the same current as the base current of the coil, ie

$$\bar{V}_{top} = -j\omega L_{es}\bar{I}_{base} \tag{7.18}$$

where L_{es} is the equivalent series inductance of the coil at the frequency ω, and the minus sign originates from our choice of current direction in figure 4.1. Eliminating $\bar{V}_{top}$ by substituting from 7.15 gives an expression for this equivalent inductance,

$$L_{es} = \frac{1}{\bar{I}_{base}} \int_0^h \int_0^h M(x,y)\bar{I}(y)\,dy\,dx \tag{7.19}$$

For coils of medium to large h/d, we find that L_{es} is typically between 70% and 100% of L_{dc}. In the case of small h/d, L_{es} can exceed L_{dc} by up to 20% due to the extra EMF induced by the current circulating through the internal capacitance - current which does not appear at the base. Addition of top-load capacitance directly to the resonator (such that the loading capacitance E-field is shared with

the coil) enhances this circulating current and therefore tends to increase the value of L_{es}. Remote capacitive loading tends to make the current profile more uniform and thus moves the L_{es}/L_{dc} ratio towards unity.

7.6. **Equivalent energy inductance.** Just as we did for the capacitance, we can form an equivalent inductance by considering the total energy stored in the magnetic field. The energy in the field which can be attributed to the mutual inductance between elements at x and y is given by

$$\begin{aligned} &M(x,y)I(x)I(y)\,dx\,dy \quad \text{if } x \neq y \\ &\frac{1}{2}M(x,x)I(x)^2\,dx^2 \quad \text{if } x = y \end{aligned} \tag{7.20}$$

and the total stored energy is the integral of 7.20 over all pairs of x and y,

$$\frac{1}{2}\int_0^h \int_0^h M(x,y)I(x)I(y)\,dx\,dy \tag{7.21}$$

We'll refer this energy to the base current by defining the *equivalent energy inductance* L_{ee} as the lumped inductor which would store the same energy if it were carrying a current I_{base}. Then we have the definition

$$L_{ee} = \frac{1}{I_{base}^2}\int_0^h \int_0^h M(x,y)I(x)I(y)\,dx\,dy \tag{7.22}$$

which amounts to a weighting of the distributed inductance by the normalised square of the current. It is found that L_{ee} is usually slightly lower than L_{es}, and the difference increases with the h/d ratio. At small h/d or high elevation, L_{ee} can exceed both L_{es} and L_{dc}. The equivalent energy inductance finds a useful application in the description the input impedance of the resonator.

8. Equivalent relationships

A number of interesting identities can be established which follow directly from the definitions of the equivalent reactances given in the previous section, which we will now illustrate using the values appropriate to the quarter-wave resonance.

To begin with, conservation of energy requires that at resonance

$$\frac{1}{2}L_{ee}I_{base}^2 = \frac{1}{2}C_{ee}V_{top}^2 \tag{8.1}$$

so that we have the relation between base current and top voltage

$$\frac{V_{top}}{I_{base}} = \sqrt{\frac{L_{ee}}{C_{ee}}} \tag{8.2}$$

This ratio is the magnitude of the *forward transfer impedance* Z_{ft} of the resonator and is seen to have a simple relationship to the equivalent energy reactances.

We also have two other relationships between base current and top voltage, this time using the phasor quantities,

$$\begin{aligned} \bar{I}_{base} &= j\omega C_{es}\bar{V}_{top} \\ \bar{V}_{top} &= -j\omega L_{es}\bar{I}_{base} \end{aligned} \tag{8.3}$$

from which we see immediately that

$$\omega = \frac{1}{\sqrt{L_{es}C_{es}}} \tag{8.4}$$

This equation is probably less useful than it may at first appear, since in order to either measure or calculate L_{es} and C_{es} it is necessary to know ω in advance. We also have for the forward transfer impedance,

$$Z_{ft} = \frac{\bar{V}_{top}}{\bar{I}_{base}} = -j\omega L_{es} = \frac{1}{j\omega C_{es}} \tag{8.5}$$

and by combining 8.5 with 8.2 we can see that

$$\omega = \frac{1}{L_{es}}\sqrt{\frac{L_{ee}}{C_{ee}}} = \frac{1}{C_{es}}\sqrt{\frac{C_{ee}}{L_{ee}}} \tag{8.6}$$

and finally we have the indentity

$$C_{ee}L_{es} = C_{es}L_{ee} \tag{8.7}$$

So far in this section and the previous, we've not said anything about the equivalent reactances when a top-load is present. All the equivalents have been defined for the bare coil only. The reader may be tempted to consider that a top-load capacitance C_{top} would simply act in parallel with C_{ee} and C_{es} when employed in equations 8.2 and 8.3, and the formulae which follow from them, but this would not be correct. There are two reasons for this. First of all the physical capacitances C_{ext} and C_{int} are modified by the nearby presence of the top-load conductor and this, together with the appearance of the toroid to coil capacitance $C_{tor}(x)$, means that the values calculated for the bare coil are no longer correct when a top-load is brought into the field. Secondly, the equivalent reactances are formed by weighting the physical reactance according to the current and voltage amplitude profiles present in the coil, and these profiles are modified by the addition of any loading. This latter problem is more serious in that the perturbation still takes place even if the electric field of the loading capacitance is far enough away from the coil field for it to be considered an independent lumped capacitance, and thereby leaving the physical coil capacitance unchanged. One way around this is to alter the definitions of the equivalent reactances to include the effect of a top-load explicitly. The resulting equivalents now relate to the resonator as a whole, rather than just the coil. The following equations summarise the revised definitions.

$$C_{dc} = C_{top} + \int_0^h C_{ext}(x)\,dx \tag{8.8}$$

$$C_{es} = C_{top} + \frac{1}{\bar{V}_{top}}\int_0^h C_{ext}(x)\bar{V}(x)\,dx \tag{8.9}$$

$$\begin{aligned} C_{ee} = C_{top} &+ \frac{1}{V_{top}^2}\int_0^h C_{ext}(x)V(x)^2\,dx \\ &+ \frac{1}{2V_{top}^2}\int_0^h\int_0^h C_{int}(x,y)(V(x)-V(y))^2\,dx\,dy \end{aligned} \tag{8.10}$$

where we understand that C_{ext}, C_{int}, $\bar{V}(x)$, and $\bar{I}(x)$ are now all to be measured or calculated with the top-load or remote lumped capacitance in place. This approach is exact, but is tantamount to admitting defeat in our stated goal of being able to use the equivalent reactances of the coil in circuit theory calculations, at least if we want to retain complete accuracy. Nonetheless, for most practical design purposes, in which a degree of approximation is usually tolerable, the equivalent

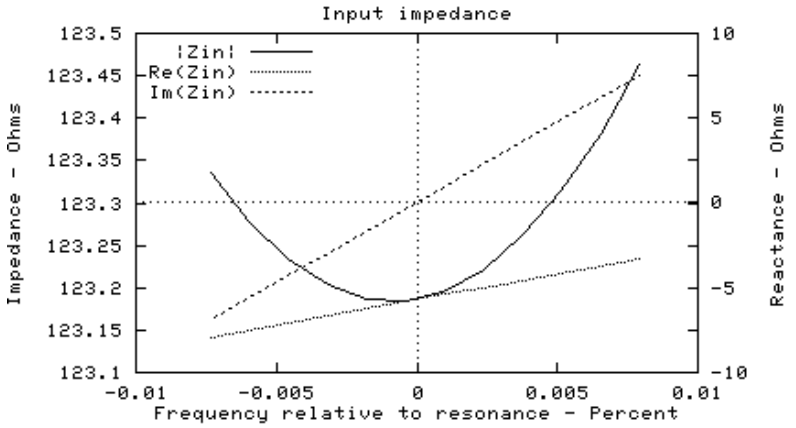

FIGURE 9.1. A close look at the input impedance near the quarter wave resonance

reactances can be taken in series or parallel with the extra reactances representing other components connected to the top of the resonator.

9. Input impedance

So far we have looked at a number of relationships involving the base current I_{base} and the top voltage V_{top} which involved equivalent reactances defined by integrals over the current and voltage distributions. These were defined for the loss-free case but retain their correctness with negligible error in the presence of the modest loss factors characteristic of Tesla secondaries. We now turn our attention to the input and output impedances, and we shall see that these are very dependent on the resonator's loss. In this section we will look at the input impedance seen when driving the coil through the base at frequencies in the vicinity of its quarter-wave resonance.

We will drive the coil by inserting an AC supply of zero source impedance in series with the base connection to the ground plane. As a result, our boundary constraint $\bar{V}(0) = 0$ which applied to the grounded base must be replaced with $\bar{V}(0) = \bar{V}_{base}$ where the phasor $\bar{V}_{base}$ describes the magnitude and phase of the input voltage. We now have the entire external circulating current of the resonator $\bar{I}_{base}$ passing through the source, and the source thus sees a complex impedance $\bar{V}_{base}/\bar{I}_{base}$. We will represent this impedance in terms of separate real and imaginary components defined by

$$Z_{in} = \frac{\bar{V}_{base}}{\bar{I}_{base}} = R_{in} + jX_{in} \tag{9.1}$$

Figure 2.1 shows the magnitude of Z_{in} in the region close to the single quarter wave resonance, together with its real and imaginary components. The frequency of resonance is defined by the point at which the imaginary component crosses zero. Below resonance, the input reactance is negative, appearing to the source as a capacitance. Above resonance the positive reactance presents an inductance to the source. At the point of resonance the input impedance is entirely real, $\bar{V}_{base}$ is in

phase with $\bar{I}_{base}$ and the source sees a load resistance R_{in}. At resonance therefore, the source must provide a real input power P_{in} given by

$$\begin{aligned} P_{in} &= \frac{|\bar{V}_{base}|^2}{R_{in}} = |\bar{I}_{base}|^2 R_{in} \\ &= \frac{V_{base}^2}{2R_{in}} = \frac{I_{base}^2 R_{in}}{2} \end{aligned} \tag{9.2}$$

in which as usual the unbarred voltage and current symbols refer to the peak amplitudes.

When the resonator is continuously supplied with energy from the AC source, the steady state equilibrium is eventually reached in which all the input power is absorbed by the resonator and the stored energy no longer increases. The loss of energy from the resonator can be described by means of a *quality factor* Q defined as usual by

$$Q = 2\pi \frac{\text{stored energy}}{\text{energy lost per cycle}} \tag{9.3}$$

If in the steady state equilibrium, energy is delivered to the resonator at a rate of P_{in} watts, then using $\frac{1}{2}C_{ee}V_{top}^2$ for the stored energy, we have

$$Q = \omega \frac{\text{stored energy}}{P_{in}} = \omega \frac{C_{ee}V_{top}^2}{2P_{in}} \tag{9.4}$$

Looking at this the other way, we can say that the input power needed to raise a peak top voltage V_{top} when driven by a continuous CW source into the base is

$$P_{in} = \omega \frac{C_{ee}V_{top}^2}{2Q} \tag{9.5}$$

We can equate equations 9.2 and 9.5 to obtain

$$P_{in} = \omega \frac{C_{ee}V_{top}^2}{2Q} = \frac{V_{base}^2}{2R_{in}} = \frac{I_{base}^2 R_{in}}{2} \tag{9.6}$$

From this we obtain a pair of identities. First we have the transfer impedance,

$$Z_{ft} = \frac{V_{top}}{I_{base}} = \sqrt{\frac{R_{in}Q}{\omega C_{ee}}} \tag{9.7}$$

which when equated with 8.2 and 8.5 gives two alternative expressions for the input resistance as a function of Q,

$$R_{in} = \frac{\omega L_{ee}}{Q} = \frac{C_{ee}}{\omega C_{es}^2 Q} \tag{9.8}$$

which demonstrates that a declining Q factor causes an increase in the apparent input resistance. A second identity obtained from 9.6 relates the base voltage to the top voltage, in other words the voltage gain,

$$\frac{V_{top}}{V_{base}} = \sqrt{\frac{Q}{\omega R_{in} C_{ee}}} \tag{9.9}$$

which, by virtue of 9.7 and 9.8 can also be written as

$$\frac{V_{top}}{V_{base}} = \frac{|Z_{ft}|}{R_{in}} = \frac{Q}{\omega} \frac{1}{\sqrt{L_{ee}C_{ee}}} \tag{9.10}$$

Since, as we mentioned in section 7, we usually have $L_{ee} < L_{es}$ and $C_{ee} < C_{es}$ for coils with medium or larger h/d, and remembering that $\omega = 1/\sqrt{L_{es}C_{es}}$, we can see that the coefficient of Q in 9.10 will usually be larger than unity, which explains why the observed voltage gain in a Tesla secondary often exceeds the value Q expected in a lumped component series LCR circuit.

Turning our attention now to the reactive component jX_{in} of the base input impedance, we can represent this reactance as the combination of an equivalent input series capacitance C_{in} and series inductance L_{in}, at least in the close neighborhood of an odd-numbered resonance ω_0, such that

$$\omega_0 = \frac{1}{\sqrt{L_{in}C_{in}}}$$
$$\text{and} \quad Z_{in}(\omega) = R_{in} + j\left(\omega L_{in} - \frac{1}{\omega C_{in}}\right) \quad ; \quad \omega \simeq \omega_0 \tag{9.11}$$

The reader may be forgiven for expecting that these input reactances would be given by the equivalent series and shunt reactances L_{es} and C_{es} defined earlier. In fact the inductance which provides a correct model of the reactive part of the coil base impedance is the equivalent energy inductance L_{ee}. We have,

$$L_{in} = L_{ee}$$
$$C_{in} = \frac{1}{\omega_0^2 L_{ee}} = \frac{L_{es}C_{es}}{L_{ee}} \tag{9.12}$$

where C_{in} is chosen so that

$$L_{in}C_{in} = L_{es}C_{es} \tag{9.13}$$

in order to satisfy the first part of 9.11. Thus, we have for the coil base input impedance in the vicinity of an odd numbered resonance at ω_0,

$$Z_{in}(\omega) = \frac{\omega_0 L_{ee}}{Q} + j\left(\omega L_{ee} - \frac{L_{ee}}{\omega L_{es}C_{es}}\right) \quad ; \quad \omega \simeq \omega_0$$
$$= \frac{\omega_0 L_{ee}}{Q}\left(1 + jy(\omega)\right) \tag{9.14}$$
$$\text{where} \quad y(\omega) = Q\left(\frac{\omega}{\omega_0} - \frac{\omega_0}{\omega}\right)$$

Note that Q will also be a function of ω, but it changes sufficiently slowly that we can regard it as constant over the domain of 9.14.

The factor $1 + jy(\omega)$ is the impedance response of the base of a lightly loaded coil near to its resonance, normalised to the impedance at resonance. At frequencies ω_+ and ω_- above and below ω_0 respectively, at which the current falls by a factor $\sqrt{2}$, the phase angle between current and voltage is 45 degrees and the magnitude of the impedance response has risen by $\sqrt{2}$. As a result, we have

$$y(\omega_+) = 1$$
$$y(\omega_-) = -1 \tag{9.15}$$

so that

$$Q\left(\frac{\omega_+}{\omega_0} - \frac{\omega_0}{\omega_+}\right) = 1$$
$$Q\left(\frac{\omega_-}{\omega_0} - \frac{\omega_0}{\omega_-}\right) = -1 \tag{9.16}$$

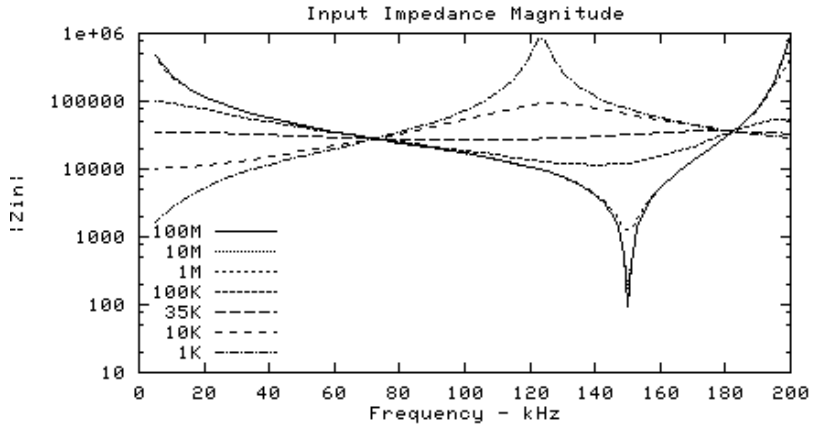

FIGURE 9.2. Input impedance magnitude as output load varies

If we divide one of the two equations 9.16 by the other, we obtain

$$\omega_-(\omega_+^2 - \omega_0^2) = \omega_+(\omega_0^2 - \omega_-^2) \tag{9.17}$$

from which we get

$$\omega_0^2 = \omega_+\omega_- \tag{9.18}$$

In other words, the resonant frequency is the geometric mean of the upper and lower $3dB$ frequencies. When we add the two equations 9.16 together, we get

$$\frac{\omega_+^2 - \omega_0^2}{\omega_+\omega_0} + \frac{\omega_0^2 - \omega_-^2}{\omega_-\omega_0} = \frac{2}{Q} \tag{9.19}$$

from which we get the usual formula relating bandwidth and Q,

$$Q = \frac{\omega_0}{\omega_+ - \omega_-} \tag{9.20}$$

The picture of the input impedance presented so far is a rather idealised one due to the use of an elementary series LCR model. In practice as increased load is applied to the resonator, the current and voltage distributions alter significantly, so that the values of the effective reactances involved in the input impedance will change. Figure 9.2 shows how the input impedance varies for a coil with an unloaded resonance at 150 kHz and a Z_{ft} of around 35kΩ. The various responses correspond to different values of load resistance applied to the top of the resonator. The highest of which, 100MΩ, results in an input impedance of 100Ω at resonance. Already, even with this modest loading, the input impedance has more than doubled from its unloaded value of around 40Ω, illustrating the extreme sensitivity of the input impedance to the load conditions. This immediately suggests the potential for difficulties when coupling power to the base of a coil under conditions where the output load resistance may vary. As further load is applied, the Q factor obviously deteriorates rapidly, and also the resonant frequency falls too. This occurs mainly because the current distribution is becoming more uniform, thereby increasing the effective inductance. Eventually, when the load resistance is about equal to the transfer impedance Z_{ft} of the resonator, the magnitude of the response is approximately flat, although generally capacitive, across the range. When the load resistance falls

below approximately Z_{ft}, the input resistance begins to resemble a parallel resonance, and the highest voltage point on the solenoid is now at the base. From the input impedance magnitude curve it appears that the quarter wave resonance is gradually dampened down, to re-emerge at a lower frequency, albeit inverted. The situation is a little more complicated than that, as can be seen from the variation of the phase angle response with the change in load resistance, as shown in figure 9.3. When the load resistance is 1MΩ and above, the phase angle crosses zero at a point close to, or a little above the frequency of minimum impedance magnitude. As the load resistance is reduced below 1MΩ down to 100kΩ the zero-phase frequency rises above the original resonant frequency, while at the same time the frequency of minimum impedance magnitude falls rapidly. Within this region, the frequency at which maximum top voltage occurs lies roughly centered between the two. As the load resistance is reduced below 100kΩ, a point is reached where the phase never does cross zero, and the impedance remains capacitive throughout the range.

These observations of the variation of input impedance with changes in load point to a number of potential difficulties likely to be encountered when driving the coil from a low impedance source at the quarter-wave frequency. To begin with, a good power-transferring match can be obtained into the low input impedance of the unloaded coil. However, as the stored energy increases, typically over many tens of cycles, a point is reached where corona or brush discharges begin to form. The energy leaked through this mechanism will appear to be dissipated in a load resistance which reduces in a non-linear way as the top voltage increases. This is reflected to the coil base as a rise in the driving point impedance, as well as a shift in the resonant frequency. The power admitted to the resonator is therefore reduced below the available source power and the net result is an equilibrium which limits further resonant rise of the stored energy. Another problem can occur when, as with most CW exciters, the operating frequency is established by a positive feedback loop responding to the coil current - a feedback which aims to set the frequency so that a certain constant total phase change, eg zero, occurs around the complete loop. We can see from the phase angle diagram that such a mechanism may get into difficulties when the load resistance has fallen to within reach of the forward transfer impedance, since there is no longer the required positive slope of phase change with frequency. In practice, a Tesla coil driven with CW is not likely to suffer a load impedance anywhere near as low as the transfer impedance as long as it is limited by brush-type discharges - the power transfer equilibrium is likely to settle at a level of discharge corresponding to a load resistance of at least several times the transfer impedance, with a loaded Q factor of order 5 or 10 at the most.

The situation is somewhat different if the resonator is able form an arc discharge to ground from the top of the coil. This typically happens while the resonator is at or approaching the brush discharge equilibrium described above. For our purposes the arc discharge instantaneously dumps the stored charge in the toploaded, and therefore resets the stored energy of the resonator to a lower level, while at the same time presenting a large step voltage transient to the top of the coil. Resonant rise then continues from the lower energy level, but now in the presence of additional decaying resonances excited by the discharge transient. As a result, in some circumstances, the CW driver may find itself acting as a load for energy reaching the base of the coil over quite a wide range of frequencies.

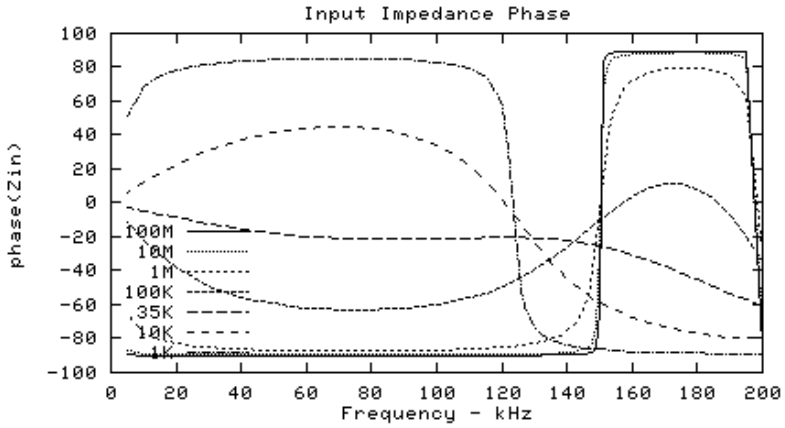

FIGURE 9.3. Input impedance phase as output load varies

10. Output Admittance

In the region of an odd-numbered resonance, the grounded-base resonator, when viewed from the top, resembles a lossy parallel resonance circuit, which we will treat as a three branch circuit by means of its admittance parameters. If we consider the coil energised through the top by means of a constant current source I_{out}, then we can describe the output admittance by the definition

$$Y_{out} = \frac{\bar{I}_{out}}{\bar{V}_{top}} = G_{out} + jS_{out} \tag{10.1}$$

where G_{out} is the output conductance, and S_{out} is the output susceptance, both being functions of ω. With CW excitation, we have the relation, complimentary to equation 9.2,

$$P_{in} = \frac{|\bar{I}_{out}|^2}{G_{out}} = \frac{I_{out}^2}{2G_{out}} = \frac{V_{top}^2 G_{out}}{2} \tag{10.2}$$

We also have, from 9.5,

$$P_{in} = \omega_0 \frac{C_{ee} V_{top}^2}{2Q} \tag{10.3}$$

which leads to the conductance

$$G_{out} = \frac{\omega_0 C_{ee}}{Q} \tag{10.4}$$

We can represent the susceptance S as

$$S_{out} = \omega C_{out} - \frac{1}{\omega L_{out}} \tag{10.5}$$

and similar argument to that used in the previous section leads us to conclude that

$$\begin{aligned} C_{out} &= C_{ee} \\ L_{out} &= \frac{1}{\omega_0^2 C_{ee}} = \frac{L_{es} C_{es}}{C_{ee}} \end{aligned} \tag{10.6}$$

so that the output admittance is

$$
\begin{aligned}
Y_{out}(\omega) &= \frac{\omega_0 C_{ee}}{Q} + j\left(\omega C_{ee} - \frac{C_{ee}}{\omega L_{es} C_{es}}\right) \quad ; \quad \omega \simeq \omega_0 \\
&= \frac{\omega_0 C_{ee}}{Q}\left(1 + jy(\omega)\right)
\end{aligned} \tag{10.7}
$$

If we invert the $Y_{out}(\omega)$ to obtain a $Z_{out}(\omega)$ we can see that the product $Z_{in}Z_{out}$ is

$$
Z_{in}Z_{out} = \frac{L_{ee}}{C_{ee}} = Z_{ft}^2 \tag{10.8}
$$

so that in a sense, Z_{ft} is the closest we have to a characteristic impedance for the solenoid at resonance.

11. Summary

We have shown how the physical reactances of the resonator can be described by distribution functions and we have applied these along with the charge conservation and the induction laws to obtain the differential equations which govern the operation of the solenoid at frequencies low enough for retardation of potentials to be ignored. The general character of the voltage and current solutions which apply to a grounded base Tesla secondary have been described, and we have given unambiguous definitions of some useful equivalent reactances. This represents a basic introduction to the physics of Tesla resonators.

Notes and References

[1] The TSSP web site at `http://www.abelian.demon.co.uk/tssp/`

[2] G. Breit, 'Distributed Capacity of Inductive Coils', Physical Review, June 1921, V17, Part 6, p649-677. See also the historical note in `http://www.abelian.demon.co.uk/tssp/misc.html`

[3] We should really be using partial differentials for these, but for the benefit of readers not too familiar with the notations of calculus we just use the ordinary differentials.

[4] An eloquent exposition on the subject of capacitance is to be found in an essay by Fred Erickson, 'The Capacitance Between Two Spheres', available in postscript from `http://www.ttc-cmc.net/~fme/spheres.11-03-99.ps.gz` which deals with the self and mutual capacitance of spheres and capacitance to infinity, using the earth-moon system as an example.

[5] Another work by Fred Erickson, 'The Non-Ideal Parallel-Plate Capacitor', which presents a highly readable introduction to the mathematical techniques of capacitance determination using the example of parallel plates to illustrate several methods. Available in postscript from `http://www.ttc-cmc.net/~fme/plates.12-24-00.ps.gz`

[6] For an example program to do this, see `http://www.abelian.demon.co.uk/tssp/model.html`

[7] See `http://www.abelian.demon.co.uk/acmi/` for a simple example of the use of current filaments to calculate the distributed mutual coupling due to a primary winding.

E-mail address: `paul@abelian.demon.co.uk`